



## Letter to the Editor

## A bulk metallic glass based on heavy rare earth gadolinium

S. Li, D.Q. Zhao, M.X. Pan, W.H. Wang \*

*Institute of Physics, Chinese Academy of Sciences, Beijing 100080, China*

Received 24 November 2004; received in revised form 4 June 2005

**Abstract**

The rare earth Gd based  $\text{Gd}_{60}\text{Al}_{10}\text{Ni}_{10}\text{Cu}_{20}$  bulk metallic glass (BMG) has been fabricated by Cu-mold casting method. The BMG-forming alloy exhibits a glass transition, obvious multi-crystallization, near eutectic melting and paramagnetic property. However, the alloy does not have a high reduced glass transition temperature ( $T_{rg} = 0.55$ ) which is a common feature for other known BMGs. We also find that a series of alloys with identical composition of  $\text{M}_{60}\text{Cu}_{20}\text{Ni}_{10}\text{Al}_{10}$  with different bases ( $\text{M} = \text{Zr}, \text{La}, \text{Nd}, \text{Pr}, \text{or Ce}$ ) can be easily cast into bulk glass. The Gd-based BMGs could have potential applications as functional materials.  
© 2005 Published by Elsevier B.V.

*PACS:* 61.43.Dq; 75.50.Kj; 64.70.Dv; 81.05.Kf

The development of bulk metallic glasses (BMGs) has received great attention because the BMGs have extraordinary structural features, unique properties and wide potential application [1–6]. A series of BMGs has been obtained based on Pd, Zr, Ti, Ni, Cu, Co, Fe, and Mg systems with a critical cooling rate less than  $10^3$  K/s for glass formation and a size with thickness more than 1 mm by conventional casting methods [1–6]. More recently, intensive efforts have been made for the fabrication of the rare-earth (RE) based BMGs because of the significance of these BMGs in science and commercial applications [7–11]. These BMGs with a low glass temperature  $T_g$  and stable supercooled liquid state offer great convenience for investigation of the nature of the glass transition, supercooled liquid and especially the metallic glass-forming melts with a large experimental accessible time and temperature window at low temperatures. On the other hand, the RE-based BMGs could have promise for application as functional materials [7–11]. However, compared to conventional metal based BMGs, only few light RE-based BMGs, such as La–

Al–Ni(Cu), Pr–Al–Ni–Cu, and Nd–Al–Fe–Co light RE-based BMGs [7,8,10,12,13], have been developed and investigated. To date, there have been few reports on the formation of RE-based BMGs in which the RE content is more than 50 at.% [13]. Gd based metallic alloys and compounds are attractive for application as functional materials because of their magnetic and magneto-optical properties. Gd-based metallic alloys with an amorphous structure also have some unique properties compared to their crystalline counterparts. For example, Gd–TM (TM = Fe, Co, Ni) metallic glassy films are of excellent magnetic cooling effect [14,15]. In this letter, we report for the first time that a heavy RE-based GdAlNiCu alloy system can be readily cast into bulk glass. The Gd-based BMG exhibits the typical glass transition and crystallization features. The glass forming ability (GFA) of the typical  $\text{Gd}_{60}\text{Cu}_{20}\text{Ni}_{10}\text{Al}_{10}$  alloy has been investigated.

Ingots with a nominal composition of  $\text{Gd}_{60}\text{Cu}_{20}\text{Ni}_{10}\text{Al}_{10}$  were prepared by arc-melting of high-purity Gd, Cu, Ni, and Al metals in a Ti-gettered argon atmosphere. The ingots were remelted several times to ensure the homogeneity of components in samples, and then were suck-cast into a copper mold under argon

\* Corresponding author. Fax: +86 10 82640223.

E-mail address: whw@aphy.iphy.ac.cn (W.H. Wang).

atmosphere to obtain a cylindrical rod 1.5–5 mm in diameter. The structure of the as-cast alloys was identified by X-ray diffraction (XRD) using a MAC M03 diffractometer with  $\text{CuK}\alpha$  radiation. The cross section of the samples was used for the XRD experiments. Thermal properties were investigated in a Perkin–Elmer differential scanning calorimeter DSC-7 and differential thermal analyzer DTA-7 under a continuous argon flow with a heating rate of 10 K/min. The values of  $T_g$  and the onset temperature for the first crystallization peak  $T_{x1}$ , were determined from DSC trace with accuracy of  $\pm 1$  K. The liquidus temperature was determined from DTA trace with accuracy of  $\pm 1$  K. The  $M$ – $H$  hysteresis loop was measured at 300 K by PPMS 6000 of Quantum Design Company, USA.

The  $\text{Gd}_{60}\text{Cu}_{20}\text{Ni}_{10}\text{Al}_{10}$  BMG rod with diameter up to 1.5 mm was prepared successfully by arc-melting and copper-mold casting. Fig. 1 shows XRD patterns of the as-cast  $\text{Gd}_{60}\text{Cu}_{20}\text{Ni}_{10}\text{Al}_{10}$  rod. The broad diffused diffraction peaks in the pattern indicate that the as-cast rod consists of mainly amorphous phase. Some weak diffraction peaks corresponding to nanocrystalline cluster are seen in the pattern. This is normal for RE-based BMG-forming alloys which usually contain 5–10% nanocrystalline particles [8]. The  $M$ – $H$  hysteresis loop of the as-cast alloy at 300 K, as shown in the inset of Fig. 1, reveals that the BMG exhibits paramagnetic property, while the other RE-based BMGs, such as  $\text{Nd}(\text{Pr})$ – $\text{Al}$ – $\text{Fe}$ – $\text{Co}$ , have hard magnetic property [7,8].

Fig. 2 presents DSC curve of the  $\text{Gd}_{60}\text{Cu}_{20}\text{Ni}_{10}\text{Al}_{10}$  BMG at a heating rate of 10 K/min. The inset is a DTA trace which shows the melting processes of the alloy. The glass transition might be sheltered by the DSC background noise. Therefore, there is a reasonable doubt if a BMG has or has not a supercooled liquid region. To eliminate the background in DSC measure-

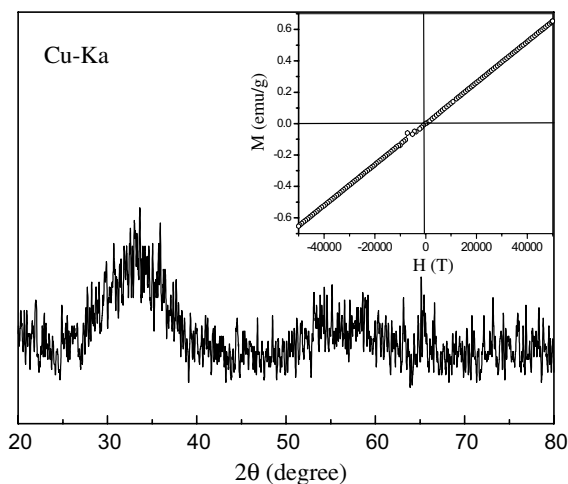


Fig. 1. XRD pattern obtained from the cross-sectional slice of the as-cast  $\text{Gd}_{60}\text{Cu}_{20}\text{Ni}_{10}\text{Al}_{10}$  BMG rod. The inset is the  $M$ – $H$  curve of the BMG conducted at 300 K.

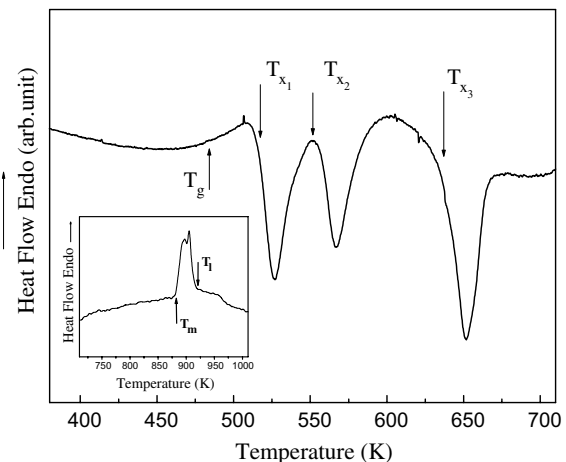


Fig. 2. DSC trace of the  $\text{Gd}_{60}\text{Cu}_{20}\text{Ni}_{10}\text{Al}_{10}$  sample showing the glass transition, crystallization, and the melting process with a cooling rate of 10 K/min.

ment, a refined DSC measurement was performed, where the same sample is measured twice: the first in the amorphous state, and then after crystallization is complete. This would allow using the curve obtained with the crystallized sample as a background, which increases the reliability of the method with regard to the elimination of the instrument background. It is found from DSC trace that this sample exhibits an obvious endothermic characteristic of the glass transition followed by three characteristic exothermic heat events indicating the successive stepwise transformations from supercooled liquid state to crystalline phases. The  $T_g$ ,  $T_{x1}$ , melting temperature,  $T_m$  and liquidus temperature,  $T_l$ , are determined to be 481, 514, 880 and 925 K, respectively. The supercooled liquid region of the alloy, defined as  $\Delta T = T_{x1} - T_g$ , is 33 K. One of the common features of the known BMGs is that they have large supercooled liquid region normally more than 50 K [1,2]. However, compared to other BMGs, the  $\text{Gd}_{60}\text{Cu}_{20}\text{Ni}_{10}\text{Al}_{10}$  BMG does not have a larger supercooled liquid region.  $\Delta T$  has been served as a parameter of the thermal stability of the supercooled liquid [16], and for some alloys, the thermal stability has a positive correlation with the GFA [17,18], but small  $\Delta T$  may not often correspond to lower GFA because the thermal stability is different from the GFA, the former indicates the resistance against the crystallization from the supercooled liquid when heating, while the GFA shows the suppression of the crystallization from the liquid in the cooling processes [19,20]. In fact, both the  $\text{La}$ – $\text{Cu}$ – $\text{Ni}$ – $\text{Al}$  and  $\text{Mg}$ – $\text{Y}$ – $\text{Cu}$ – $\text{Ag}$ – $\text{Pd}$  BMGs with a 12 mm diameter rod reported only have small value of  $\Delta T$  of 29 and 32 K, respectively [20]. This leads to the preexisting cluster in the BMGs. These crystalline clusters will continue to grow as soon as  $T_g$  is reached, and then markedly reduced the value of  $\Delta T$ .

The reduced glass transition temperature  $T_{rg} = T_g/T_m$  [12], which is a critical parameter in determining the glass forming ability of an alloy, is 0.55, and smaller than 2/3 that is an empirical criterion for BMG formation. From the endothermal signal of the melting, one can see that this multi-component alloy is very close eutectic point. The distinct glass transition, near-eutectic melting, and obvious crystallization events further confirm the amorphous phase of the BMG.

Fig. 3 exhibits XRD patterns of the  $Gd_{60}Cu_{20}Ni_{10}Al_{10}$  alloy quenched with different cooling rates. When the diameter of the cast rod is larger than 1.5 mm, there are crystalline peaks on the diffused peak that indicating that these rod samples are a mixture of amorphous and crystalline phases. The critical cooling rates for the full glass formation of the alloy can be estimated by using:  $dT/dt$  (K/s) =  $10/R^2$  (cm) [21], where  $R$  is the typical dimension of the formed amorphous alloy. For the  $Gd_{60}Cu_{20}Ni_{10}Al_{10}$  alloy, its critical cooling rate is about 500 K/s. The precipitation crystalline phases for the rod with  $\phi = 2$  mm are identified as hexagonal  $Al_3Gd$  and other unidentified phases as indicated in Fig. 3. With decreasing cooling rate, more crystalline phases like cubic  $AlNi$ , and cubic  $Al_2$  tetragonal  $Al_2Gd_3$  and cubic  $AlGd$  are also found. The precipitation of crystalline phases is different with the decreasing of cooling rate. Fig. 4 shows XRD patterns taken from the as-cast rod with  $\phi = 1.5$  mm for the  $GdCuNiAl$  alloy with different compositions. Except for the  $Gd_{60}Cu_{20}Ni_{10}Al_{10}$ , the altering of atomic ratio of multicomponent  $Gd-Cu-Ni-Al$  alloy leads to the appearance of crystalline phases in amorphous matrix. The replacement of  $Cu$  by  $Fe$  does also not improve its GFA. The  $Gd-Cu-Ni-Al$  BMG has a small composition range compared to other known BMGs.

It is known that the BMG-forming alloys are very sensitive to their components and composition [1,2]. Surprisingly, we found that a series of different BMGs

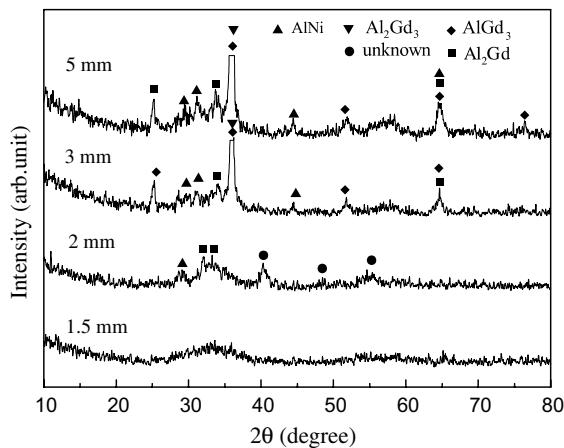


Fig. 3. XRD patterns of the  $Gd_{60}Cu_{20}Ni_{10}Al_{10}$  alloy quenched with the different cooling rates.

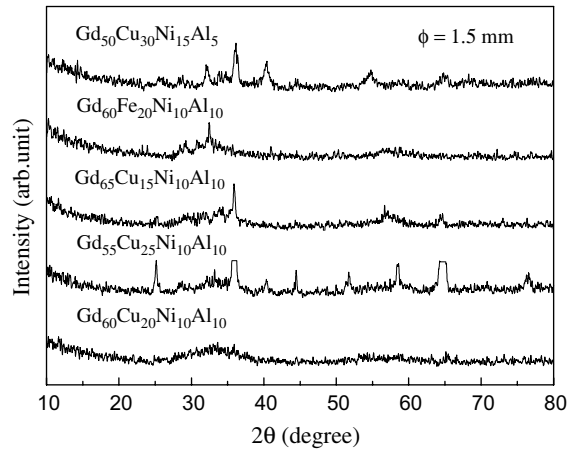


Fig. 4. XRD patterns taken from the as-cast 1.5 mm diameter of  $Gd_{60}Cu_{20}Ni_{10}Al_{10}$ ,  $Gd_{55}Cu_{25}Ni_{10}Al_{10}$ ,  $Gd_{65}Cu_{15}Ni_{10}Al_{10}$ ,  $Gd_{60}Cu_{20}Ni_{10}Al_{10}$ , and  $Gd_{50}Cu_{30}Ni_{15}Al_5$  BMG rods.

with the same composition of  $M_{60}Cu_{20}Ni_{10}Al_{10}$  ( $M = Zr, La, Nd, Pr, \text{ or } Ce$ ) can also be obtained by conventional casting. The multicomponent alloys have excellent GFA when other various element ( $Zr, La, Nd, Pr, \text{ or } Ce$ ) is selected as the base element instead of  $Gd$ . Table 1 lists thermodynamic parameters of  $T_g$ ,  $T_{x1}$ ,  $\Delta T$ ,  $T_m$ , and  $T_{rg}$  for the various obtained BMGs. It seems that  $M_{60}Cu_{20}Ni_{10}Al_{10}$  represents a special composition point for BMG formation. It is worth to note that the atomic weight of the RE has obvious effect on the glass forming ability of the alloys. The  $La$ -based alloy with the lightest atomic weight of  $La$  has the best GFA, the  $Gd$  is of the highest atomic weight, and the  $Gd$ -based alloy has poorest GFA in these RE based BMG-forming alloys. The mechanism is not clear yet, and more work is needed.

In conclusions, the heavy  $Gd$ -based  $Gd_{60}Cu_{20}Ni_{10}Al_{10}$  BMG with a good GFA is obtained by conventional  $Cu$ -mold casting method. We report that the other alloys has identical composition of  $M_{60}Cu_{20}Ni_{10}Al_{10}$  ( $M = Zr, La, Nd, Pr, \text{ or } Ce$ ) can also be cast into BMG.  $Gd$  is an important RE element with magnetic properties. So the  $Gd$ -based BMGs could have unique properties and have potential applications as a

Table 1  
Thermodynamic parameters of  $M_{60}Cu_{20}Ni_{10}Al_{10}$  ( $M = Gd, La, Nd, Pr, \text{ or } Ce$ )

BMGs	$T_g$ (K)	$T_{x1}$ (K)	$\Delta T$ (K)	$T_m$ (K)	$T_{rg}$
$Gd_{60}Cu_{20}Ni_{10}Al_{10}$	481	514	33	880	0.55
$La_{60}Cu_{20}Ni_{10}Al_{10}$	387	447	60	694	0.56
$Pr_{60}Cu_{20}Ni_{10}Al_{10}$	413	461	48	708	0.58
$Ce_{60}Cu_{20}Ni_{10}Al_{10}$	374	441	67	645	0.58
$Nd_{60}Cu_{20}Ni_{10}Al_{10}$	438	478	40	728	0.60
$Zr_{41}Ti_{14}Cu_{12.5}Ni_{10}Be_{22.5}$	623	680	57	941	0.66
$Pd_{40}Ni_{10}Cu_{30}P_{20}$	582	718	95	804	0.72

For comparison, the typical  $Pd_{40}Ni_{10}Cu_{30}P_{20}$  and  $Zr_{41}Ti_{14}Cu_{12.5}Ni_{10}Be_{22.5}$  BMGs are also presented.

functional material as well. Related properties studies are in progress.

### Acknowledgment

The authors are grateful for the financial support of the National Science Foundation of China (Grant Nos. 50321101, 50371097 and 50371098).

### References

- [1] A. Inoue, Bulk Amorphous Alloys: Preparation and Fundamental Characteristics, Trans Tech, Switzerland, 1998.
- [2] W.H. Wang, C. Dong, C.H. Shek, Mater Sci. Eng. R44 (2004) 45.
- [3] Z.P. Lu, C.T. Liu, Phys. Rev. Lett. 91 (2003) 115505.
- [4] V. Ponnambalam, S.J. Poon, G.J. Shiflet, Appl. Phys. Lett. 83 (2003) 1131.
- [5] W.L. Johnson, MRS Bull. 24 (1999) 42.
- [6] W.H. Wang, Q. Wei, H.Y. Bai, Appl. Phys. Lett. 71 (1997) 58.
- [7] B.C. Wei, W.H. Wang, M.X. Pan, B.S. Han, Phys. Rev. B 64 (2001) 012406.
- [8] Z. Zhang, R.J. Wang, B.C. Wei, W.H. Wang, Appl. Phys. Lett. 81 (2002) 4371.
- [9] F.Q. Guo, S.J. Poon, G.J. Shiflet, Appl. Phys. Lett. 83 (2003) 2575.
- [10] Z.F. Zhao, D.Q. Zhao, W.H. Wang, Appl. Phys. Lett. 82 (2003) 4699.
- [11] H. Tan, Y. Zhang, D. Ma, Y.P. Feng, Y. Li, Acta Mater. 51 (2003) 4551.
- [12] A. Inoue, T. Zhang, T. Masumoto, Mater. Trans. JIM 30 (1989) 965.
- [13] A. Inoue, T. Zhang, T. Masumoto, Mater. Trans. JIM 31 (5) (1990) 425.
- [14] X.Y. Liu, J.A. Barclay, T.K. Bose, J. Combe, J. Appl. Phys. 79 (1996) 1630.
- [15] P. Liu, Q.Q. Yang, Y.S. Yang, Electrochim. Acta 45 (2000) 2147.
- [16] T.A. Waniuk, J. Schroers, W.L. Johnson, Appl. Phys. Lett. 78 (2001) 1213.
- [17] Y. Zhang, D.Q. Zhao, M.X. Pan, W.H. Wang, Mater. Trans. JIM 41 (2000) 1423.
- [18] A. Inoue, T. Zhang, T. Masumoto, J. Non-Cryst. Solids 156–158 (1993) 473.
- [19] J. Schroers, A. Masuhr, W.L. Johnson, R. Busch, Phys. Rev. B 60 (1999) 11855.
- [20] K. Amiya, A. Inoue, Mater. Trans. 42 (2001) 543.
- [21] X.H. Lin, W.L. Johnson, J. Appl. Phys. 78 (1995) 6514.